

Influence of the symmetry of the hybridization on the critical temperature of multi-band superconductors

Daniel Reyes,^{1,*} Nei Lopes,² Mucio A. Continentino,² and Christopher Thomas³

¹*Instituto Militar de Engenharia - Praça General Tibúrcio, 80, 22290-270, Praia Vermelha, Rio de Janeiro, Brazil*

²*Centro Brasileiro de Pesquisas Físicas, Rua Dr. Xavier Sigaud 150, Urca, 22290-180, Rio de Janeiro, Brazil*

³*Departamento de Física, Universidade Federal Rural do Rio de Janeiro, 23897-000, Seropédica, Rio de Janeiro, Brazil*

(Dated: December 29, 2021)

In this work we study a two-band model of a superconductor in a square lattice. One band is narrow in energy and includes local Coulomb correlations between its quasi-particles. Pairing occurs in this band due to nearest neighbor attractive interactions. Extended s -wave, as well as d -wave symmetries of the superconducting order parameter are considered. The correlated electrons hybridize with those in another, wide conduction band through a k -dependent mixing, with even or odd parity depending on the nature of the orbitals. The many-body problem is treated within a slave-boson approach that has proved adequate to deal with the strong electronic correlations that are assumed here. Since applied pressure changes mostly the ratio between hybridization and bandwidths, we can use this ratio as a control parameter to obtain the phase diagrams of the model. We find that for a wide range of parameters, the critical temperature increases as a function of hybridization (pressure), with a region of first-order transitions. When frustration is introduced it gives rise to a stable superconducting phase. We find that superconductivity can be suppressed for specific values of band-filling due to the Coulomb repulsion. We show how pressure, composition and strength of correlations affect the superconductivity for different symmetries of the order parameter and the hybridization.

I. INTRODUCTION

Many superconducting materials of current interest are multi-band systems, with electrons from different atomic orbitals coexisting at a common Fermi surface. This is the case of heavy fermions and high T_c superconductors, either based on Cu or Fe . Therefore, to take into account the multi-band character seems to be essential to understand the physical properties of these superconductors.

In the materials we are interested, we can distinguish two different types of electronic quasi-particles. One is associated with nearly localized electrons in a narrow band, and another consists of conduction electrons in a wide band¹⁻⁴. The admixture between these distinct quasi-particles is responsible for many of the properties of multi-band systems, such as, their magnetism and response functions.

A model to describe these materials must consider these features and take into account the local Coulomb repulsion among the electrons in the narrow d (cuprates, pnictides) or f (heavy fermions) bands. The most favorable conditions for the appearance of superconductivity involve an attractive interaction that pairs quasi-particles of the narrow band in neighboring sites avoiding in this way the strong on-site Coulomb repulsion. This type of pairing entails different symmetries of the superconducting order parameter. Experimentally, it is well known that in the case of the cuprates, they adopt a d -wave symmetry and on-site pairing vanishes.

An interesting experimental fact observed in multi-band superconductors is the existence of a quantum phase transition associated with a superconducting quan-

tum critical point (SQCP)⁵⁻⁷. Varying an external control parameter, such as doping or pressure, these systems can be driven to a non-superconducting metallic state or even to an insulator⁸. Notice that the ratio between hybridization and bandwidth, which depends on the overlap of different wave functions is sensitive to these external parameters. Consequently, theoretical phase diagrams⁸⁻¹⁴ obtained as a function of this ratio have a direct resemblance to those obtained experimentally when pressure or doping is varied^{5-7,15-17}. It turns out that in realistic cases, the parity of the hybridization is very important. In multi-band systems we have in general to consider the mixing of s - p , s - f , p - d , p - f and d - f orbitals, which hybridize with different parities^{18,19}.

The motivation of this work is to investigate how quantities, such as, the critical temperature vary as a function of the different parameters of the model. Specifically, we consider the intensity and symmetry of the hybridization, the occupation of the bands and the strength of the local repulsion.

We shall apply the slave-boson (SB) mean-field approach to solve the many-body problem. This is a well-known technique to deal with the type and magnitude of the electronic correlation that we are interested. We perform a self-consistent numerical solution of a set of coupled equations to obtain finite temperature phase diagrams. These present regions of metastability, i.e., of first-order transitions that mainly occur whenever the critical temperature increases as a functions of hybridization. We show that if frustration effects are taken into account the superconducting phase can be stabilized in these regions. We find that Coulomb interactions can suppress superconductivity, for specific values of band-

filling.

We point out that our approach does not aim to describe any specific material, but to provide a general guide to expectations of how different control parameters affect the properties of multi-band superconductors when different symmetries of the hybridization and order parameter are considered.

The paper is organized as follows: in section II we present the model, with its main features required to describe a multi-band superconductor with a narrow band of strongly correlated electrons. We also introduce in this section the SB formalism used to treat the many-body problem. In section III we show and discuss our results for both, zero and finite temperature phase diagrams as a function of hybridization, band-filling and Coulomb repulsion. Finally, in section IV we point out the main results.

II. THE MODEL

We consider a two-dimensional (2D), two-band lattice model with inter-site attractive interactions and local Coulomb repulsion between electrons in the narrow band, which we refer generically as *f-electrons*. These can be either *d-electrons* as for the *Cu* or *Fe* superconductors, or *f-electrons* as for the actinides and rare-earth heavy fermions. This narrow band hybridizes with a conduction band of *c-electrons* through a *k*-dependent hybridization that can have different symmetries.

The Hamiltonian of the model is given by⁸,

$$\begin{aligned} \mathcal{H} = & \sum_{k,\sigma} \epsilon_k^c c_{k,\sigma}^\dagger c_{k,\sigma} + \sum_{k,\sigma} \epsilon_k^f f_{k,\sigma}^\dagger f_{k,\sigma} \\ & + \sum_{k,\sigma} (V_k c_{k,\sigma}^\dagger f_{k,\sigma} + h.c.) + U \sum_i f_{i,\uparrow}^\dagger f_{i,\uparrow} f_{i,\downarrow}^\dagger f_{i,\downarrow} \\ & + \frac{1}{2} \sum_{\langle ij \rangle, \sigma} J_{ij} f_{j,\sigma}^\dagger f_{j,-\sigma}^\dagger f_{i,-\sigma} f_{i,\sigma}, \end{aligned} \quad (2.1)$$

where $c_{k,\sigma}^\dagger$ ($c_{k,\sigma}$) and $f_{k,\sigma}^\dagger$ ($f_{k,\sigma}$) are creation (annihilation) operators related to conduction and *f*-electrons with spin σ in the wide uncorrelated band, and in the narrow band, respectively.

These bands are described by the dispersion relations, ϵ_k^c and ϵ_k^f , for *c* and *f*-electrons in an obvious notation. Since we do not consider magnetic solutions these dispersions are independent of the spin σ . U is the on-site repulsive interaction ($U > 0$) among the *f*-electrons. The two types of electrons are hybridized, with a *k*-dependent matrix element V_k ¹⁴. The last term describes an effective attraction between *f*-electrons in neighboring sites ($J_{ij} < 0$) and is responsible for superconductivity²⁰. It takes into account, experimental results for the specific heat in multi-band superconductors that show unequivocally that *f*-electrons are involved in the pairing²¹. Notice that this term also describes antiferromagnetic (AF), *xy*-type exchange interactions between these electrons,

such that magnetic and superconducting ground states are in competition. In this work we are only interested in the latter. We have also neglected in this interaction an Ising term that when decoupled in the superconducting channel leads to *p*-wave pairing that is not considered here.

It is worth to point out that all terms in Eq. (2.1) can vary substantially from one specific class of systems to another. In particular, the interactions J_{ij} should be small for the case of rare-earth heavy fermions due to the localization of the *f*-orbitals in these systems. We have glossed over inter-band attractive interactions among the *c* and *f*-electrons and intra-band attractive interactions between *c*-electrons since they do not affect the superconducting order parameter in a drastic way²⁰. Also inter-band pair hopping²² that arises in second order in the hybridization when applying a Schrieffer-Wolff transformation for the Anderson lattice model is ruled out, since it gives rise not only to ground states with finite *q*-pairing states but also to anisotropic *s*-wave superconductivity²³.

The Hamiltonian, Eq. (2.1) represents a model that considers the basic features of a multi-band superconductor with a narrow band of strongly correlated electrons. It reflects a difficult many-body problem and has been treated using different approximations. Several approaches have been used depending on the different aspects of the problem that one wants to emphasize. This includes, competition between different ground states²⁴, superconducting properties at zero or finite temperature^{25,26}, *c-f*-pairing²³ or the nature of the phase diagram as a function of the occupation of the bands.

In this work, we approach this complicated many-body problem using the mean-field slave boson formalism^{27–29}, which has been shown suitable for studying coexistence between superconductivity and magnetism²⁵, crossover from BCS-type to local pairing³⁰, magnetic instabilities^{31–33}, and the effect of infinite^{11,34,35} and finite^{8,20,36} Coulomb repulsion in narrow bands. It has also been shown to be in remarkable agreement with more elaborated numerical Monte Carlo results over a wide range of interactions and particle densities³⁷.

Considering a finite on-site Coulomb repulsion U in the SB formalism, each lattice site one can have four physical states. The empty state $|0\rangle$, the states where there is one *f*-electron with a given spin $|\uparrow\rangle$ and $|\downarrow\rangle$ and the doubly occupied configuration $|\uparrow\downarrow\rangle$, such that the total number of *f*-electrons per site, n_f can be $n_f = n_{i\uparrow}^f + n_{i\downarrow}^f = 0, 1$ or 2 . In order to describe all these states that *f*-electrons can occupy, it is introduced four bosons e , d , p_\uparrow , and p_\downarrow , where e , d are associated with empty and doubly occupied sites, respectively, and the boson p_\uparrow (p_\downarrow) with a singly occupied site with spin component \uparrow (\downarrow)²⁹.

For the purpose of establishing a one-to-one correspondence between the original Fock space and the enlarged one that also contains the bosonic states, the constraints $e_i^\dagger e_i + p_{i,\uparrow}^\dagger p_{i,\uparrow} + p_{i,\downarrow}^\dagger p_{i,\downarrow} + d_i^\dagger d_i = 1$ for the completeness of the bosonic operators, and $f_{i\sigma}^\dagger f_{i\sigma} = p_{i\sigma}^\dagger p_{i\sigma} + d_i^\dagger d_i$, for the local particle (boson+fermion) conservation at the *f*

sites, must be satisfied. Such constraints are imposed in each site by the Lagrange multipliers λ_i and $\alpha_{i,\sigma}$, respectively.

In the physical sub-space, the operators $f_{i,\sigma}$ are mapped, such that, $f_{i,\sigma} \rightarrow f_{i,\sigma} Z_{i,\sigma}$ where $Z_{i,\sigma} = \frac{(e_i^\dagger p_{i,-\sigma} + p_{i,\sigma}^\dagger d_i)}{\sqrt{(1-d_i^\dagger d_i - p_{i,\sigma}^\dagger p_{i,\sigma})(1-e_i^\dagger e_i - p_{i,-\sigma}^\dagger p_{i,-\sigma})}}$ and where the square root term ensures that the mapping becomes trivial at the mean-field level in the non-interacting limit ($U \rightarrow 0$). The usual procedure consists in taking a mean-field approach where we assume the slave bosons to be condensed^{8,20,32}. Then all bosons operators are replaced by their expectation values as, $Z = \langle Z_{i,\sigma}^\dagger \rangle = \langle Z_{i,\sigma} \rangle = Z_\sigma$, $e = \langle e_i \rangle = \langle e_i^\dagger \rangle$, $p_\sigma = \langle p_{i,\sigma} \rangle = \langle p_{i,\sigma}^\dagger \rangle$, and $d = \langle d_i \rangle = \langle d_i^\dagger \rangle$. Due to translation invariance these expectation values take the same value on all sites.

Using this approximation the Hamiltonian Eq. (2.1) can be written as,

$$\begin{aligned} \mathcal{H}_{eff} = & \sum_{k,\sigma} (\epsilon_k^c - \mu) c_{k,\sigma}^\dagger c_{k,\sigma} + \sum_{k,\sigma} (\tilde{\epsilon}_k^f - \mu) f_{k,\sigma}^\dagger f_{k,\sigma} \\ & + \sum_{k,\sigma} ZV_k (c_{k,\sigma}^\dagger f_{k,\sigma} + h.c.) \\ & + \frac{Z^2}{2} \sum_{k,\sigma} (\Delta \eta_k f_{k,\sigma}^\dagger f_{-k,-\sigma}^\dagger + h.c.) - N \frac{|\Delta|^2}{J} \\ & + \lambda \sum_{k,\sigma} (p_\sigma^2 + p_{-\sigma}^2) - \alpha \sum_{k,\sigma} (p_\sigma^2 + d^2) \\ & + N\lambda(e^2 + d^2 - 1) + NUd^2, \end{aligned} \quad (2.2)$$

where N is the number of lattice sites and $\Delta = \frac{Z^2 J}{N} \sum_k \eta_k \langle f_{-k,-\sigma}^\dagger f_{k,\sigma} \rangle$ represents the superconducting order parameter for extended s or d -wave symmetries^{38,39}, since the strong Coulomb repulsion prevents local s -wave pairing between f -electrons. η_k denotes any of the possible pairing symmetries $\cos k_x + \cos k_y$ and $\cos k_x - \cos k_y$ for s and d waves, respectively.

It is worth to point out that we obtain, for both symmetries, stable superconducting states in different parameter regions, while most of the authors have studied only d -wave superconductivity in the presence of strong local repulsive interactions^{40,41}. We also have added in the Hamiltonian, Eq. (2.1), the chemical potential μ that has to be adjusted when we fix the total band-filling, $n = n_s + n_f$ at different values. We assume a nearest neighbor, constant attractive interaction $J_{ij} = J$. For simplicity, we consider a square lattice with $\epsilon_k^c = -2t(\cos k_x + \cos k_y)$ and $\epsilon_k^f = \epsilon_0^f + \gamma \epsilon_k^c$, where $\gamma = t_f/t$ ($\gamma < 1$) is the ratio of hopping terms of the quasi-particles in different bands and ϵ_0^f is the bare f -band center. Furthermore, we introduce $\tilde{\epsilon}_k^f = \epsilon_k^f + \alpha$ as the renormalized dispersion of the f -band. We took the lattice parameter $a = 1$.

We use the Green's function method^{8,39}, such that the excitations in the superconducting phase are given by the poles of these Green's functions, which in turn are obtained from their equations of motion. These excitations

have energy given by $\pm\omega_{1,2}$, where,

$$\omega_{1,2} = \sqrt{A_k \pm \sqrt{B_k}} \quad (2.3)$$

$$\begin{aligned} A_k = & \frac{\epsilon_k^{c2} + \epsilon_k^{f2}}{2} + \tilde{V}_k^2 + \frac{(\tilde{\Delta}\eta_k)^2}{2}, \\ B_k = & \left(\frac{\epsilon_k^{c2} - \epsilon_k^{f2}}{2} \right)^2 + \tilde{V}_k^2 (\epsilon_k^c + \epsilon_k^f)^2 + \frac{(\tilde{\Delta}\eta_k)^4}{4} \\ & - \frac{(\tilde{\Delta}\eta_k)^2}{2} (\epsilon_k^{c2} - \epsilon_k^{f2}) + (\tilde{\Delta}\eta_k \tilde{V}_k)^2, \end{aligned} \quad (2.4)$$

with, $\tilde{V}_k = ZV_k$, $\tilde{\Delta} = Z^2\Delta$, $\epsilon_k^c = \epsilon_k^c - \mu$, and $\epsilon_k^f = \tilde{\epsilon}_k^f - \mu$.

The effect of the hybridization's parity on the superconducting properties^{42,43}, is considered assuming an odd-parity hybridization $\tilde{V}_{-k} = -\tilde{V}_k$ with $\tilde{V}_k = iZV(\sin k_x + \sin k_y)$, and an even-parity hybridization, such that, $\tilde{V}_{-k} = \tilde{V}_k$ with $\tilde{V}_k = ZV(\cos k_x + \cos k_y)$. The former case is relevant when the orbitals involved in the mixing have angular momenta differing by an odd number, as p - d or d - f , whereas the latter case is considered when the difference in angular momenta is even¹⁸. For completeness, we also consider a constant k -independent hybridization. In all cases, V represents the intensity of the hybridization.

Following the slave boson mean-field approximation, the parameters e , p , d , α and λ , are obtained from the minimization of the Hamiltonian, given by Eq. (2.2)⁸, with respect to the different slave-boson parameters. This procedure yields a set of coupled equations that has to be solved self-consistently together with the number and gap equations. The last two are given by,

$$\begin{aligned} n = & 1 + \frac{1}{N} \sum_k \sum_{\ell=1,2} \frac{(-1)^\ell}{2\sqrt{B_k}} \frac{1}{2\omega_\ell} \\ & \times \left\{ (\epsilon_k^c + \epsilon_k^f) \left(\omega_\ell^2 + \tilde{V}_k^2 - \epsilon_k^c \epsilon_k^f \right) - \tilde{\Delta}^2 \eta_k^2 \epsilon_k^c \right\} \\ & \times \tanh \left(\frac{\beta\omega_\ell}{2} \right), \end{aligned} \quad (2.5)$$

$$\frac{1}{J} = \frac{Z^4}{N} \sum_k \sum_{\ell=1,2} \frac{\eta_k^2 (-1)^\ell}{2\sqrt{B_k}} \left(\frac{\omega_\ell^2 - \epsilon_k^{c2}}{2\omega_\ell} \right) \tanh \left(\frac{\beta\omega_\ell}{2} \right), \quad (2.6)$$

respectively. In this equations $\beta = 1/k_B T$, where k_B is the Boltzmann constant and T is the absolute temperature.

The self-consistent numerical solution of the set of coupled equations described above, allows us to obtain the critical superconducting temperature T_c for different occupations of the bands and types of hybridization. Assuming that the intensity of the latter can be controlled by external pressure, we obtain the pressure dependence of T_c for different symmetries and electronic occupations.

III. ANALYSIS OF RESULTS

The numerical solution of the self-consistent coupled equations allows us to obtain both the zero and finite temperature phase diagrams of the model for different cases⁸. We consider the influence of the parity of the hybridization for both extended s -wave and d -wave symmetries of the superconducting order parameter, which are referred as Δ_s or s -wave and Δ_d , respectively. In all figures below, we take $\epsilon_0^f = 0$, and the ratio of the effective masses $\gamma = 0.1$. For this choice of $\epsilon_0^f = 0$ and before turning on the interactions and hybridizations, the half-filled band case corresponds to $\mu = 0$. Furthermore, we renormalize all the physical parameters by the c -band hopping term $t = 1$.

A. Zero temperature results

The zero temperature density plots for the extended s -wave order parameter are shown in Fig. 1 as a function of

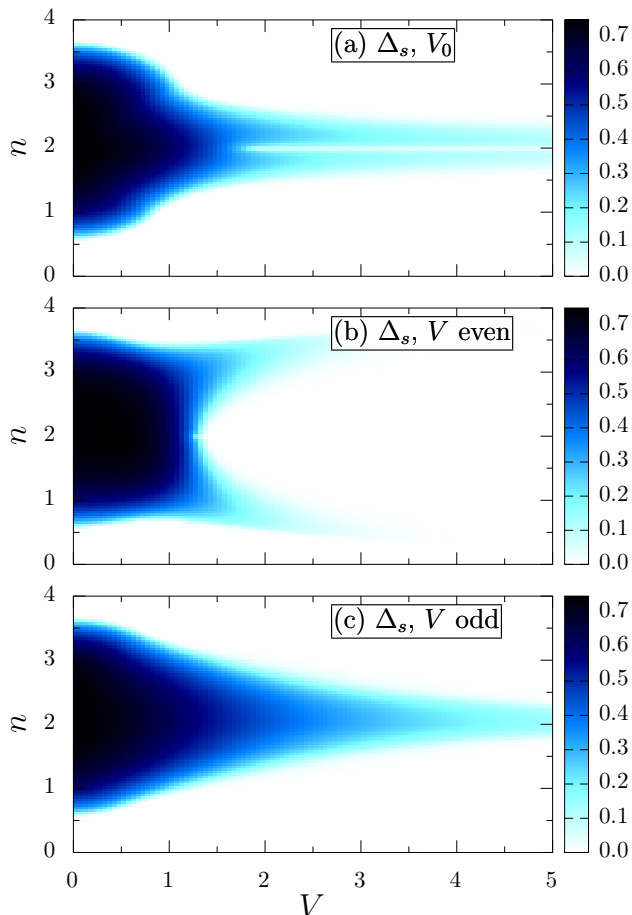


FIG. 1. (Color online) Density plots of Δ_s varying n and V , for fixed values of attractive interaction $J = -2$ and a Coulomb repulsion $U = 1$. Figs. 1(a), 1(b) and 1(c) are sketched considering a constant⁸, even and odd-parity hybridizations, respectively.

the intensity of hybridization for different band-fillings. Fig. 1(a), Fig. 1(b) and Fig. 1(c) consider the cases of constant ($V = V_0$), even and odd-parity hybridization, respectively.

Fig. 2 shows the same density plots, but now for the case of a d -wave order parameter, as a function of the intensity of hybridization and different band-fillings. Fig. 2(a), Fig. 2(b) and Fig. 2(c) consider constant⁸, even and odd-parity hybridizations, respectively.

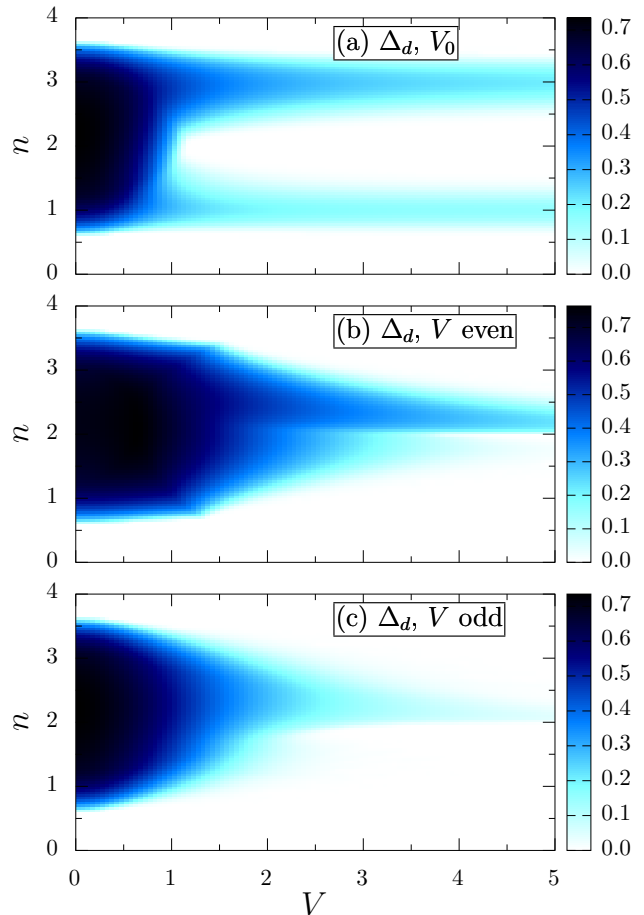


FIG. 2. (Color online) Density plots of Δ_d varying n and V , for fixed values of attractive interaction $J = -2$ and a Coulomb repulsion $U = 1$. Figs. 2(a), 2(b) and 2(c) are sketched considering a constant⁸, even and odd-parity hybridization, respectively.

The influence of the symmetry of the hybridization is notable in the figures, for both cases of d and extended s -wave superconductivity. For extended s -wave, it is remarkable, in the case of even hybridization, the existence of a critical value of hybridization that suppresses superconductivity. Also the regions of superconductivity are almost symmetric with respect to the half-filling $n = 2$, independent of the parity of the hybridization, which is not the case for d -wave superconductivity. For d -wave and odd hybridization the phase diagram, Fig. 2(c), is very similar to that of Ref. 44 obtained using a full variational Gutzwiller wave function incorporating non-local

effects of the on-site interaction. Then, in spite of the very different approaches, the results they yield are in qualitative agreement.

B. Finite temperatures

Next, we consider the temperature dependence of the self-consistent equations and solve for the superconducting critical temperature (T_c) of the model as a function of different parameters. Since T_c is the most accessible experimental quantity and many of the model parameters can be tuned, the calculation of T_c provides a direct test of the results. Besides, since we are studying a non-trivial two-band model, in which superconductivity coexists with strong local correlations and competes with the hybridization between the bands, the study of the effect of each of these features in T_c turns out to be very important. Therefore, in this section we investigate the dependence of the critical temperature T_c on the parity of the hybridization, band-filling and the repulsive interaction for each specific symmetry of the superconducting (SC) order parameter.

1. The critical temperature as function of the hybridization

First, we show the results for T_c as a function of hybridization for different band-fillings and parities of the mixing. We consider both cases, of extended s -wave (Fig. 3) and d -wave (Fig. 4) symmetries of the superconducting order parameter.

For consistency, we check our results with those for the case of constant hybridization and extended s -wave symmetry (Fig. 3(a)) that has been calculated previously²⁰. The behavior of T_c that we obtain agrees qualitatively with that in the literature²⁰. In Fig. 3(b) and Fig. 3(c), as well as in Fig. 4(b) and Fig. 4(c), we show our new results for the critical temperature for different parities of the mixing between the bands and several occupations. Fig. 3 shows the behavior of the critical temperature for a s -wave superconducting order parameter as a function of the parity of the hybridization and different band-fillings. Fig. 4 shows the same results for T_c , but now for a d -wave superconducting order parameter. It is interesting that even for a rather *dilute* case $n = 0.5$, superconductivity arises for large values of an even hybridization ($V > 2$), see Fig. 3(c). For larger band-fillings, the superconducting phase appears for all V symmetries and remains for occupations up to $n \approx 3.5$.

One can see from Fig. 3 and Fig. 4 that, except for $n \approx 0.5$ and $n \approx 3.5$, there is a region in the phase diagrams where the critical temperatures increase with increasing the intensity of hybridization from small V . This type of behavior has been seen in previous works²⁰. In order to understand the physics behind this increase, we have studied the behavior of the free energy³⁰ as a function of the superconducting order parameter in the

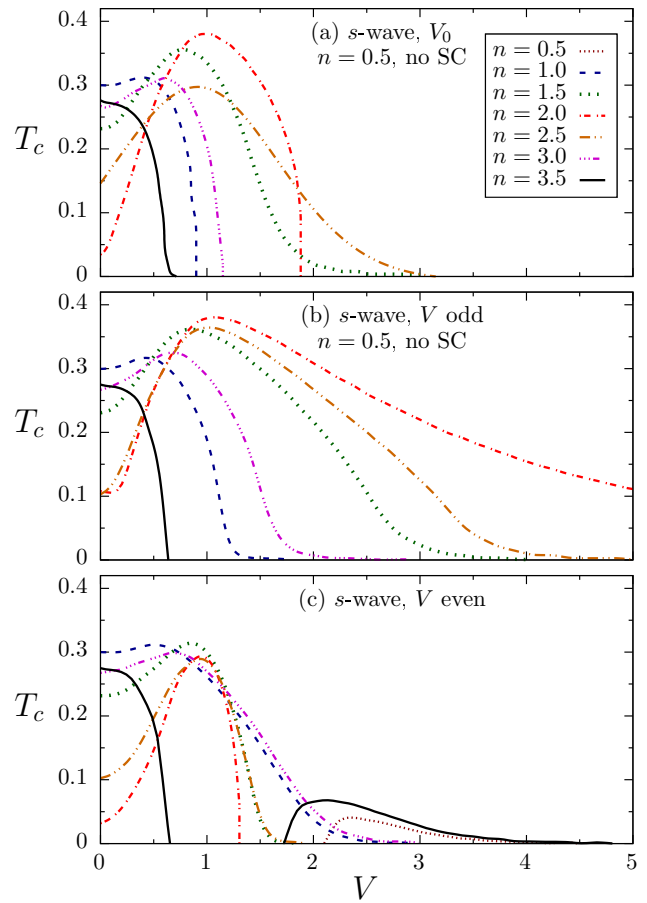


FIG. 3. (Color online) T_c as a function of different V symmetries considering an extended s -wave SC order parameter for fixed values of attractive interaction $J = -2.0$ and Coulomb repulsion $U = 1.0$. Figs. 3(a), 3(b) and 3(c) are sketched for several values of the band-filling n , considering a constant, odd and even-parity hybridization, respectively (see text).

regions of the phase diagrams where this enhancement of T_c is observed.

Fig. 5 shows the free energy as a function of the extended s -wave order parameter Δ_s , for a fixed temperature $T = 0.25$ and $n = 1.5$, varying the intensity of the even hybridization from $V = 0.1$ to $V = 1.2$ (see also Fig. 3(c)). One can see the presence of minima (arrow), located at zero and finite Δ_s , that exchange stability as the intensity of the even parity hybridization increases. For small values of V , the stable phase is the normal metal with $\Delta_s = 0$, although one can already notice the presence of two metastable minima for finite Δ_s . As V reaches $V \approx 0.4$ the three minima become degenerate and the system enters in the superconducting phase through a first-order transition.

First-order transitions between normal and superconducting states have already been obtained in strongly correlated systems⁴³ using a Kondo lattice approach. Here, we obtain coexistence between these states in a two-band

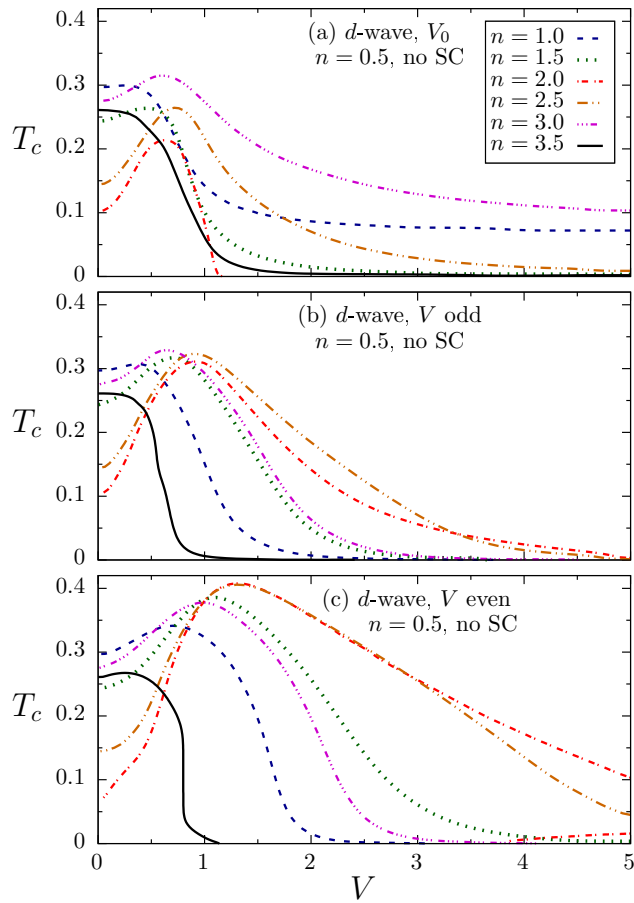


FIG. 4. (Color online) T_c as a function of different V symmetries considering a d -wave SC order parameter, for fixed values of attractive interaction $J = -2.0$ and Coulomb repulsion $U = 1.0$. Figs. 4(a), 4(b) and 4(c) are sketched for several values of the band-filling n , considering a constant, odd and even-parity hybridization, respectively (see text).

model. Experimentally, first-order transitions have been reported in compounds that present spin-triplet superconductivity^{45,46} and in pnictides, where structural and magnetic first-order phase transitions occur for a characteristic temperature^{47,48}.

For $V \approx 0.4$ there is an exchange of stability between the normal and superconducting phases. Further increase of the value of V takes the system smoothly, through a second-order transition, to the normal phase. In general, we can conclude that in the regions of the phase diagram that T_c increases with V the system is metastable and presents a first-order phase transition and coexistence of phases. The actual phase diagram obtained from an analysis of the free energy as a function of the superconducting order parameter is shown in Fig. 6. The shaded region represents the place of coexistence. This kind of behavior, i.e., first-order transitions for small V , up to the maxima in the T_c versus V curves will be present for all symmetries. However, another notable feature

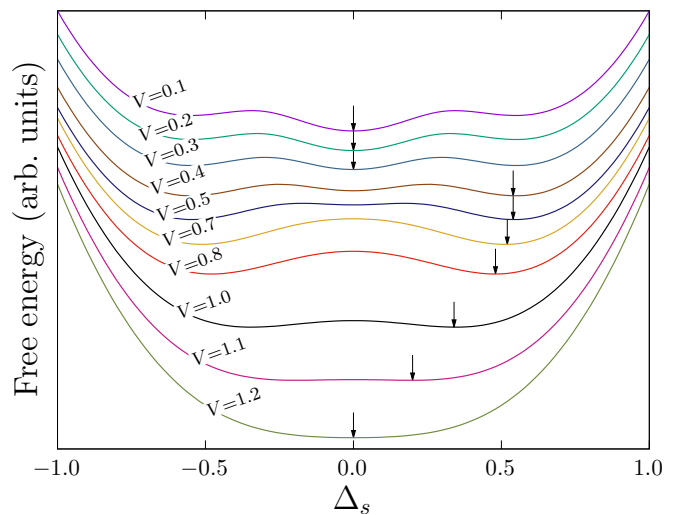


FIG. 5. (Color online) Free energy variation for different values of Δ_s . The minimum (arrow) can be seen floating abruptly and then smoothly when we fix $T = 0.25$, $n = 1.5$, and we vary V (see text).

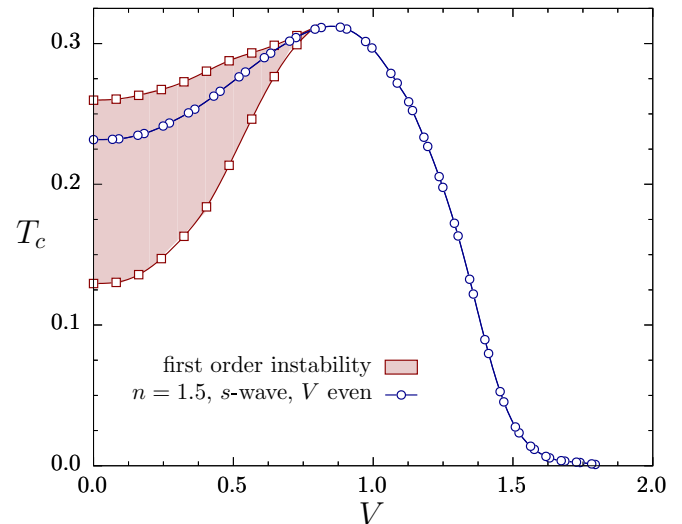


FIG. 6. (Color online) Phase diagram showing T_c as a function of even parity hybridization for extended s -wave SC order parameter. The curves are obtained from plots of the free energy as in Fig. 5. The shaded area represents the region of phase coexistence.

worth to emphasize is that the first-order region, associated with the existence of maxima in T_c versus V curve, is suppressed for small and large band-fillings. In fact for $n \lesssim 0.5$ and $n \gtrsim 3.5$, we no longer observe maxima in T_c as a function of V for any symmetry (see Fig. 3 and Fig. 4), and consequently we have only second-order transitions. Our numerical results show that the local Coulomb repulsion decreases the region in the phase diagram where the system presents first-order transitions,

but does not suppress it. In practice, we observe that the maxima in the T_c versus V curves shifts to smaller values of V with increasing Coulomb repulsion. It is worth noticing in Fig. 3(c), for V even and large band-filling ($n = 3.5$), the presence of two superconducting *domes* as a function of V , unlike for constant (Fig. 3(a)) or odd (Fig. 3(b)) parity of the hybridization.

Finally, we remark that for d -wave symmetry, Fig. 4, we observe a different behavior from that of the extended s -wave case. First, for $n = 0.5$, there is no SC for any parity of the hybridization and second we find no evidence of two superconducting domes for V even and large occupations, as in the previous case of extended s -wave superconductivity. On the other hand, the first-order transitions remain present for small V associated with a region of the phase diagram where T_c increases with V , the intensity of hybridization. Once again, this instability region is suppressed as n increases. The effect of increasing the local U is similar to the extended s -wave case and independent of the parity of V , i.e., the instability region decreases, but is not suppressed.

The model investigated here also supports antiferromagnetic solutions for similar values of the parameters²⁵. This magnetic phase competes with superconductivity in the same region of the phase diagram. In multi-band systems as heavy fermions, superconductivity arises in proximity to an antiferromagnetic quantum critical point⁴⁹. In order to verify whether these two phases actually compete or antiferromagnetic fluctuations enhance superconductivity, we introduced frustration in our model⁴². This is done by including a constant hybridization $V_0 = 1$ and a nearest neighbor symmetric mixing $V(\cos k_x + \cos k_y)$

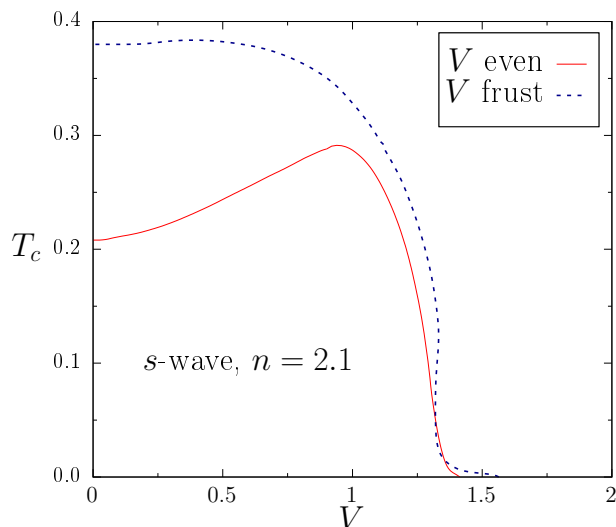


FIG. 7. (Color online) T_c as a function of hybridization for the cases of no frustration (continuous line) and increasing frustration (dashed line) for a band-filling of $n = 2.1$ and extended s -wave pairing and fixed values of attractive interaction $J = -2$ and Coulomb repulsion $U = 1$ (see text).

of varying intensity (see Fig. 7).

We find that increasing frustration enhances and stabilizes superconductivity, at least for small V , as expected if this is in competition with antiferromagnetism. Fig. 7 shows T_c for a band-filling $n = 2.1$, in the cases of a pure even hybridization (no frustration) (continuous line) of intensity V and when this competes with a constant one of unit intensity, $V_0 = 1$ (dashed line). In the former case the transition to the superconducting state is first order below the maximum, as shown by an analysis of the free energy (see Fig. 6). As frustration is included, T_c increases and the transition becomes second order, such that, frustration stabilizes the superconducting state⁴².

2. The critical temperature as function of the band-filling

Next, we show our results for the critical temperature as a function of band-filling, for different intensities and parities of the hybridization and distinct symmetries of the order parameter. Our results agree qualitatively, when available, with those obtained previously²⁰. In Fig. 8 and Fig. 9, we show the finite temperature phase diagrams for different symmetries of the order parameter as a function of band-filling for different parities of the hybridization. The Coulomb repulsion is kept fixed at $U = 1$. The phase diagrams for each symmetry depend strongly on the parity of \tilde{V}_k . In general, superconductivity does not occur for small number of particles or holes. In some cases the critical temperature is a maximum for half-filled bands, while for others it is suppressed in this case.

An analysis of the free energy curves as a function of the band-filling n shows that for small values of the intensity of the hybridization, $V \leq 1$, independent of its parity and symmetry of the superconducting order parameter, superconductivity becomes metastable for $1.0 \leq n \leq 3.0$. For $V \geq 1$ coexistence of phases disappears and superconductivity is stable when T_c is finite.

The results of Fig. 8 for extended s -wave symmetry of the order parameter are closely related to those of Fig. 1. In particular we remark that for odd parity hybridization, i.e., Fig. 8(b), the critical temperature attains a maximum for band-filling $n = 2$, while for V even it is mostly suppressed for this occupation, even giving rise to two separate regions of superconductivity, see Fig. 8(c). It is a general feature in Fig. 8 that increasing the intensity of hybridization, shrinks the region of superconductivity in the phase diagram.

The results for d -wave symmetry of the order parameter are shown in Fig. 9, and are closely associated to those of Fig. 2. In this case, we notice that the phase diagram is in general asymmetric with respect to half-occupation of the bands ($n = 2$), specially for large V . For $n < 2$ and in both cases of even and odd parity, large intensities of the hybridization suppress superconductivity as can be seen in Fig. 9(c) and Fig. 9(b), respectively. The values of T_c in this case are significantly higher for even parity

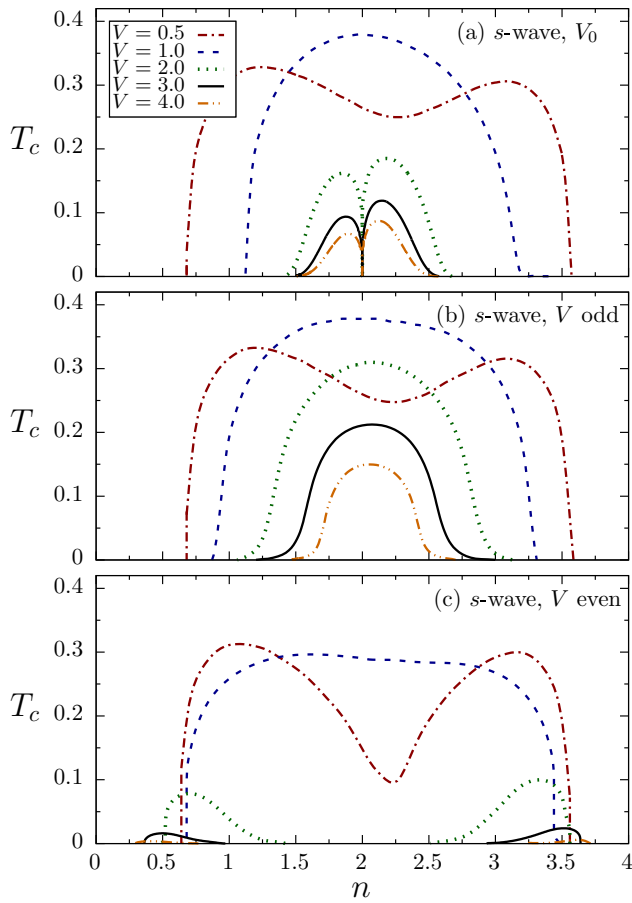


FIG. 8. (Color online) T_c as a function of band-filling n considering an extended s -wave SC order parameter. This plot is shown for fixed values of attractive interaction $J = -2$ and Coulomb repulsion $U = 1$. Figs. 8(a), 8(b) and 8(c) are sketched for several values of intensity of V , considering a constant, odd and even-parity hybridization, respectively (see text).

hybridization. For large, k -independent V , we see again the presence of two superconducting domes.

3. The critical temperature as function of the Coulomb correlation

Finally, we discuss the effect of the local Coulomb correlation U on superconductivity. We start with the case of an extended s -wave superconductor where the critical temperatures as a function of U are shown in Fig. 10 for fixed intensity of hybridization ($V = 1$). In general, the critical temperature decreases smoothly with increasing local Coulomb repulsion. Remarkably, this is not always the case. For large band-fillings, the critical temperature may increase with U and then be strongly suppressed with further increase giving rise to a superconducting quantum critical point.

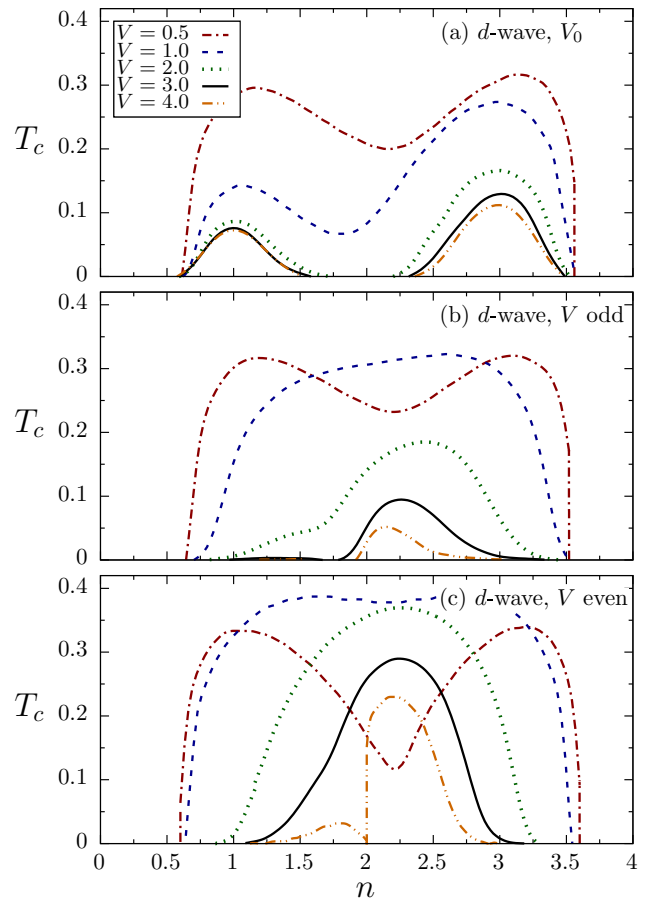


FIG. 9. (Color online) T_c as a function of band-filling n considering a d -wave SC order parameter. This plot is shown for fixed values of attractive interaction $J = -2$ and Coulomb repulsion $U = 1$. Figs. 9(a), 9(b) and 9(c) are sketched for several values of intensity of V , considering a constant, odd and even-parity hybridization, respectively (see text).

Our numerical results for constant k -independent hybridization are in qualitative agreement with those obtained previously²⁰ for extended s -wave symmetry and large U . Here we extend the calculations for a larger range of band-fillings, for different parities of the hybridization and different symmetries of the superconducting order parameter. Also we consider the case of small U that has not been studied before. This is probably the most interesting, since it can give rise to an increase of T_c , for sufficiently large occupations.

We further remark in Fig. 10, that for small band-filling $n = 0.5$ there is no SC order and also for $n = 1.0$ with V constant, see Fig. 10(a). As we increase n , the finite critical temperature decreases with increasing U , but remains finite for large U for specific values of band-filling ($n \leq 2.0$). However, for large band-filling $n = 3.0$, we see a very different behavior, i.e., T_c increases and then is suppressed with increasing U . Note that T_c for even parity V , Fig. 10(c), is rather lower than for the

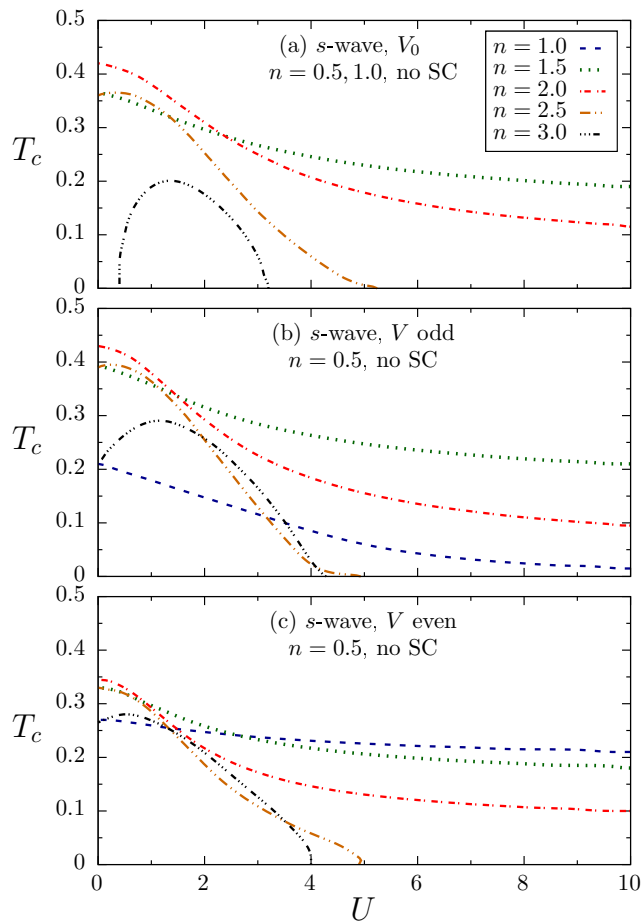


FIG. 10. (Color online) T_c as a function of U considering an extended s -wave SC order parameter. This plot is shown for fixed values of attractive interaction $J = -2$ and $V = 1.0$. Figs. 10(a), 10(b) and 10(c) are sketched for several values of n , considering a constant, odd and even-parity hybridization, respectively (see text).

other cases.

For d -wave symmetry Fig. 11 shows results not very different from the extended s -wave case. For small band-filling $n = 0.5$ there is no SC order for any parity of V . As we increase n the SC order appears and T_c decreases, but remains finite for large U only for specific values of band-filling. In contrast with extended s -wave symmetry, now the higher T_c is obtained for V even. Here, we also observe an increase of T_c with band-filling, but there is no longer any T_c dome for the same range of parameters. Finally, we point out that a stability analysis of the free energy shows that superconductivity, depicted in Fig. 10 and Fig 11 as a function of increasing local repulsion and for $V \geq 1$ is always stable. The phase transitions shown in these figures are continuous, second-order transitions.

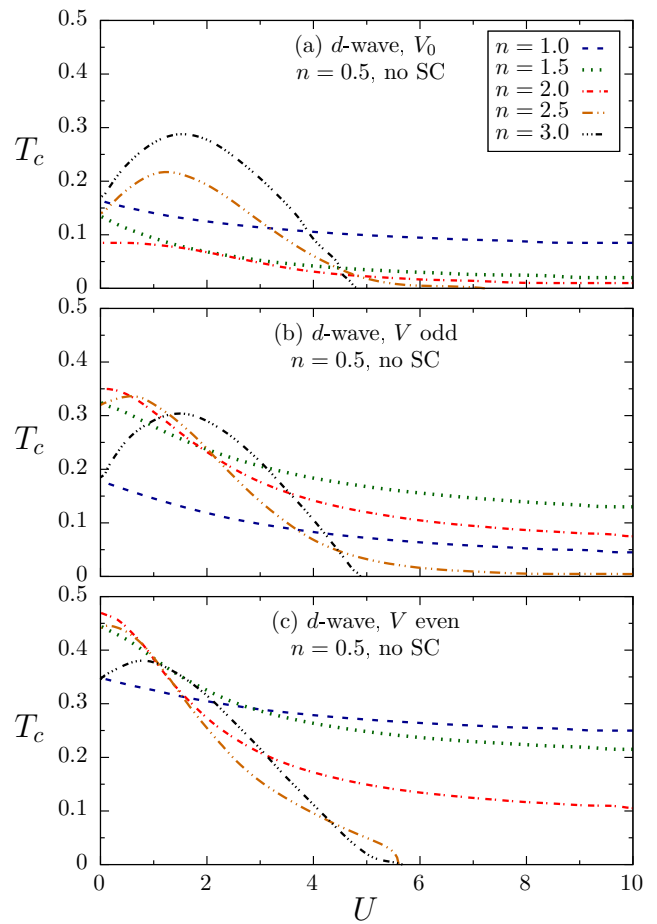


FIG. 11. (Color online) T_c as a function of U considering a d -wave SC order parameter. This plot is shown for fixed values of attractive interaction $J = -2$ and $V = 1.0$. Figs. 11(a), 11(b) and 11(c) are sketched for several values of n , considering a constant, odd and even-parity hybridization, respectively (see text).

IV. CONCLUSIONS

In this work, we have studied a two-band model for a superconductor in a square lattice. Electronic correlations in the narrow band were treated using a slave boson approach. We have obtained the superconducting order parameter and the critical temperature of the model as a function of the band-filling, hybridization and Coulomb repulsion for both extended s -wave and d -wave symmetries. We considered the cases of even and odd hybridizations with respect to inversion symmetry. A superconducting phase is found for all cases, and in some of them, a superconducting quantum critical point is obtained.

For band-fillings between $n \approx [1.0 : 3.0]$, the critical temperature increases as hybridization increases, reaching a maximum and then decreases. This initial increase for small V is generally associated with a metastable character of the superconducting state and the presence

of first-order transitions in this region of the phase diagram. When frustration effects are included, the critical temperature no longer increases and the superconducting phase is *stabilized*.

We found that the critical temperature is strongly dependent on the band-filling. For instance, for $n \approx 0.5$, as well as $n \approx 3.5$ and even symmetry of hybridization, two superconducting regions are obtained: one with the usual initial decrease of the superconducting critical temperature with V and a *second* with a dome for higher values of hybridization. The Coulomb repulsion is also an important ingredient affecting superconductivity: for certain values of band-filling it can lead to a suppression of the superconducting phase, instead of a continuous asymptotic decrease as reported in previous works^{8,20}.

We expect that our results can be useful as a guide to expectations for the finite temperature properties of multi-band superconductors. The behavior of the critical temperature with external parameters that can be

controlled experimentally, together with the theoretical insights that we have obtained can provide a useful criterion to distinguish between different symmetries of the order parameter and the nature of the orbitals involved in the superconductivity.

V. ACKNOWLEDGMENTS

M.A.C. would like to thank the Brazilian agencies FAPERJ, CAPES and CNPq for partial financial support. N.L. would like to thank to CNPq for doctoral fellowship. D.R. would like to thank the Brazilian Center for Research in Physics (CBPF) where part of this work was done. Finally, we would like to thank COTEC (CBPF), since the numerical calculations were performed on the *Cluster HPC*.

-
- * daniel@cbpf.br
- ¹ R. Micnas, J. Ranninger, and S. Robaszkiewicz, *Rev. Modern Phys.* **62**, 113 (1990).
 - ² S. Robaszkiewicz, R. Micnas, and J. Ranninger, *Phys. Rev. B* **36**, 180 (1987).
 - ³ A. C. Hewson, *The Kondo Problem to Heavy Fermions*, Cambridge University Press, Cambridge, UK, (1993).
 - ⁴ P. Gegenwart, Q. Si, and F. Steglich, *Nat. Phys.* **4**, 186 (2008).
 - ⁵ S. M. Ramos, M. B. Fontes, E. N. Hering, M. A. Continentino, E. Baggio-Saitovich, F. D. Neto, E. M. Bittar, P. G. Pagliuso, E. D. Bauer, J. L. Sarrao, J. D. Thompson, *Phys. Rev. Lett.* **105**, 126401 (2010).
 - ⁶ K. Jin, N. P. Butch, K. Kirshenbaum, J. Paglione, R. L. Greene, *Nature*, **476** 73 (2011).
 - ⁷ K. Jin, N. P. Butch, K. Kirshenbaum, J. Paglione, R. L. Greene, *Proc. Natl. Acad. Sci.* **109** 8440 (2012).
 - ⁸ Daniel Reyes, Claudine Lacroix, Christopher Thomas and M. A. Continentino, *Annals of Physics*, **373**, 257 (2016).
 - ⁹ M. A. N. Araújo, N. M. R. Peres, and P. D. Sacramento, *Phys. Rev. B* **65**, 012503 (2001).
 - ¹⁰ N. M. R. Peres and M. A. N. Araújo, *J. Phys.: Condens. Matter*, **14**, 5575 (2002).
 - ¹¹ L. P. Oliveira and P. D. Sacramento, *Phys. Rev. B* **66**, 014516 (2002).
 - ¹² Akihisa Koga and Philipp Werner, *J. Phys. Soc. Japan* **79** (11), 114401 (2010).
 - ¹³ Akihisa Koga and Philipp Werner, *J. Phys.: Conf. Ser.* **302**, 012040 (2011).
 - ¹⁴ Daniel Reyes and M. A. Continentino *Solid State Communications* **205**, 19 (2015).
 - ¹⁵ Eduardo H. da Silva Neto, Riccardo Comin, Feizhou He, Ronny Sutarto, Yeping Jiang, Richard L. Greene, George A. Sawatzky, Andrea Damascelli, *Science* **347** 282 (2015).
 - ¹⁶ E. D. Bauer, F. Ronning, C. Capan, M. J. Graf, D. Vandervelde, H. Q. Yuan, M. B. Salamon, D. J. Mixson, N. O. Moreno, S. R. Brown, J. D. Thompson, R. Movshovich, M. F. Hundley, J. L. Sarrao, P. G. Pagliuso, S. M. Kauzlarich, *Phys. Rev. B* **73**, 245109 (2006).
 - ¹⁷ E. D. Bauer, N. O. Moreno, D. J. Mixson, J. L. Sarrao, J. D. Thompson, M. F. Hundley, R. Movshovich, P. G. Pagliuso, *Physica B* **359**, 35 (2005).
 - ¹⁸ Fernanda Deus, Mucio A. Continentino, and Heron Caldas, *Annals of Physics* **362**, 208 (2015).
 - ¹⁹ Heron Caldas, F. S. Batista, Mucio A. Continentino, Fernanda Deus, and David Nozadze, *Annals of Physics* **384**, 224 (2017).
 - ²⁰ P. D. Sacramento, J. Aparício and G. S. Nunes, *J. Phys.: Condens. Matter* **22**, 065702 (2010).
 - ²¹ P. Coleman, *Handbook of Magnetism and Advanced Magnetic Materials* **1**, 95 (2007).
 - ²² Katsuro Hanzawa and Kei Yosida, *J. Phys. Soc. Japan* **56**, 3440 (1987).
 - ²³ Keisuke Masuda and Daisuke Yamamoto, *Phys. Rev. B* **87**, 014516 (2013).
 - ²⁴ Mohammad Zhian Asadzadeh, Michele Fabrizio, and Federico Becca, *Phys. Rev. B* **90**, 205113 (2014).
 - ²⁵ P. D. Sacramento, *J. Phys.: Condens. Matter* **15** 6285 (2003).
 - ²⁶ Michał Zegrodnik and Józef Spałek, *New J. Phys.* **20**, 063015 (2018).
 - ²⁷ P. Coleman, *Phys. Rev. B* **29**, 3035 (1984).
 - ²⁸ P. Coleman, *Phys. Rev. B* **35**, 5072 (1987).
 - ²⁹ G. Kotliar and A. E. Ruckenstein, *Phys. Rev. Lett.* **57**, 1362 (1986).
 - ³⁰ Bogdan R. Bulka and Stanisław Robaszkiewicz, *Phys. Rev. B* **54**, 13138 (1996).
 - ³¹ Peter, Woelfle, *J. Low Temp. Phys.* **99**, 3/4, 625 (1995).
 - ³² V. Dorin and P. Schlottmann *Phys. Rev. B* **46**, 10800 (1992).
 - ³³ J. Aparício, G. S. Nunes, and P. D. Sacramento, *Journal of Physics: Conference Series* **150**, 042144 (2009).
 - ³⁴ M. A. N. Araújo, N. M. R. Peres, P. D. Sacramento and V. R. Vieira, *Phys. Rev. B* **62**, 9800 (2000).
 - ³⁵ N. M. R. Peres, P. D. Sacramento, and M. A. N. Araújo *Phys. Rev. B* **64**, 113104 (2001).
 - ³⁶ V. Dorin and P. Schlottmann *Phys. Rev. B* **47**, 5095 (1993).

- ³⁷ L. Lilly, A. Muramatsu, and W. Hanke, *Phys. Rev. Lett.* **65**, 1379 (1990).
- ³⁸ Andrzej Ptok, David Crivelli, and Konrad Jerzy Kapcia, *Supercond. Sci. Technol.* **28**, 045010 (2015).
- ³⁹ D. Reyes, M. A. Continentino, F. Deus and C. Thomas, *J. Phys.: Condens. Matter*, **30**, 18 (2018).
- ⁴⁰ J. Spalek, *Phys. Rev. B* **38**, 208 (1988).
- ⁴¹ O. Howczak, J. Kaczmarczyk, and J. Spalek, *Phys. Stat. Solidi (b)* **250**, 609 (2013).
- ⁴² Wei Wu and A. M.-S. Tremblay, *Phys. Rev. X* **5**, 011019 (2015).
- ⁴³ Heidrun Weber and Matthias Vojta, *Phys. Rev. B* **77**, 125118 (2008).
- ⁴⁴ Marcin M. Wysokiński, Jan Kaczmarczyk, and Jozef Spalek, *Phys. Rev. B* **94**, 024517 (2016).
- ⁴⁵ Shingo Yonezawa Tomohiro Kajikawa, and Yoshiteru Maeno, *Phys. Rev. Lett.* **110**, 077003 (2013).
- ⁴⁶ Shunichiro Kittaka, Akira Kasahara, Toshiro Sakakibara, Daisuke Shibata, Shingo Yonezawa, Yoshiteru Maeno, Kenichi Tenya, and Kazushige Machida, *Journal of Magnetism and Magnetic Materials*, **400**, 81 (2016).
- ⁴⁷ Shiliang Li, Clarina de la Cruz, Q. Huang, Y. Chen, J. W. Lynn, Jiangping Hu, Yi-Lin Huang, Fong-Chi Hsu, Kuo-Wei Yeh, Maw-Kuen Wu, and Pengcheng Dai, *Phys. Rev. B* **79**, 054503 (2009).
- ⁴⁸ P. S. Wang, S. S. Sun, Y. Cui, W. H. Song, T. R. Li, Rong Yu, Hechang Lei, and Weiqiang Yu, *Phys. Rev. Lett.* **117**, 237001 (2016).
- ⁴⁹ N. D. Matur, F. M. Grosche, S. R. Julian, I. R. Walker, D. M. Freye, R. K. W. Haselwimmer and G. G. Lonzarich, *Nature* **394**, 39 (1998).